Eco-Engineered Silver-Diatomite Nanocomposites from Agro-Industrial Waste for Sustainable Antibacterial Agent: A Combined Laboratory and Molecular Simulation Study

Saprini Hamdiani
Department of Chemistry, Faculty of Mathematics and Natural Science, University of Mataram

Iwan Sumarlan
Department of Chemistry, Faculty of Mathematics and Natural Science, University of Mataram

Evana
Research Center for Pharmaceutical Ingredients and Traditional Medicine, Research Organization for Health, National Research and Innovation Agency

Saprizal Hadisaputra
Chemistry Education Division, University of Mataram

他

https://doi.org/10.5109/7402627

出版情報：Evergreen. 12 (4), pp.1946-1960, 2025-12. Interdisciplinary Graduate School of Engineering Sciences, Kyushu University, Japan
バージョン：

Eco-Engineered Silver-Diatomite Nanocomposites from Agro-Industrial Waste for Sustainable Antibacterial Agent: A Combined Laboratory and Molecular Simulation Study

Saprini Hamdiani[1,*], Iwan Sumarlan[1], Evana[2], Saprizal Hadisaputra[3], Siti Raudhatul Kamali[4], Yeng-Fong Shih[5]

[1]Department of Chemistry, Faculty of Mathematics and Natural Science, University of Mataram, Indonesia
[2]Research Center for Pharmaceutical Ingredients and Traditional Medicine, Research Organization for Health, National Research and Innovation Agency, Cibinong, Indonesia
[3]Chemistry Education Division, University of Mataram, Indonesia
[4]Department of Environmental Science, Faculty of Mathematics and Natural Sciences, University of Mataram, Indonesia
[5]Department of Applied Chemistry, Chaoyang University of Technology, Taichung, Taiwan

*Author to whom correspondence should be addressed:
E-mail: saprini.h@unram.ac.id

(Received April 28, 2025; Revised August 02, 2025; Accepted September 13, 2025)

Abstract: This study addresses the growing need for sustainable and effective antibacterial agents amid rising antibiotic resistance. We developed eco-friendly silver-natural diatomite nanocomposites (Ag-NDs) from agro-industrial waste using pineapple leaf (PL) extract. The methods employed included a green one-pot synthesis using pineapple leaf extract, which resulted in AgNP-NDs-PL; a conventional calcination method, which produced AgNP-NDs-Calc; and molecular simulation to support the experimental findings. The resulting nanocomposites materials were characterized by Fourier Transform Infrared Spectroscopy (FTIR), Particle Size Analysis (PSA), X-ray Diffraction (XRD), Scanning Electron Microscopy–Energy Dispersive X-ray Spectroscopy (SEM-EDX), Thermogravimetric Analysis (TGA), and Transmission Electron Microscopy (TEM) analyses, followed by antibacterial assays and molecular simulation. The molecular simulations were performed using the Material Studio 7.0 with the calculation of adsorption energies between five major phytochemical constituents in pineapple leaf extract on (Ag(100)) surface. The AgNp-NDs-PL nanocomposites synthesized by green synthesis showed superior antibacterial activity at lower silver concentrations against *Pseudomonas aeruginosa* and *Staphylococcus aureus* due to smaller nanoparticle size and phytochemical synergy. Complementary molecular simulations revealed that strong interactions between Ag(100) and 1,3-O-dicaffeoylglycerol from pineapple leaf extract. This integrated experimental-computational approach offers a novel, sustainable strategy for fabricating potent antibacterial agents aligned with circular economy principles.

Keywords: Agro-industrial waste; Antibacterial; Molecular Simulation Natural Diatomite Waste; Silver Nanoparticles

1. Introduction

The increasing emergence of antibiotic-resistant bacteria poses a critical threat to public health, prompting the urgent development of sustainable and effective antibacterial agents. In recent years, nanomaterials, especially silver-based nanoparticles (AgNPs) have garnered considerable attention for their potent antimicrobial properties, broad-spectrum activity, and long-term stability[1,2]. However, conventional chemical and physical synthesis methods often involve toxic reagents and energy-intensive processes, contradicting the principles of green chemistry[3,4]. To address this challenge, eco-friendly synthesis approaches utilizing renewable resources and waste materials have become a major focus in materials science and sustainable nanotechnology[5].
Agro-industrial and mineral-based wastes offer abundant,

Cite: S. Kamali et al., "Eco-Engineered Silver-Diatomite Nanocomposites from Agro-Industrial Waste for Sustainable Antibacterial Agent: A Combined Laboratory and Molecular Simulation Study". Evergreen, 12 (04) 1946-1960 (2025). https://doi.org/10.5109/7402627.

low-cost, and biodegradable resources that can be valorized for functional nanomaterial production. Among these, pineapple leaves, an underutilized agricultural byproduct rich in phytochemicals, can serve as natural reducing and stabilizing agents for nanoparticle synthesis[6,7]. However, the synthesis of nanoparticles by using agricultural byproduct has significant challenges to maintain the nanoscale size in nanoparticle solution[8]. The sizes of nanoparticles synthesized using pineapple leaf extract solution exhibited instability after being stored at room temperature for seven days[9]. To increase its stability, organic and inorganic material has been employed as a host for a nanoparticle's growth[10]. Organic hosts such as natural fibers from *Thespesia lampas*[11] and eggshell powder[12] have been applied; however, these materials typically suffer from fragility and low thermal stability at elevated temperatures. In contrast, inorganic hosts such as zeolite[13,14], diatomite[15,16], clay[17-19], and montmorillonite[20] offer superior thermal resistance and structural stability. In addition, the inorganic material offers high mechanical strength, and porous structure, making them effective in preventing nanoparticle agglomeration. Similarly with agricultural byproduct, natural diatomite, a siliceous mineral derived from fossilized diatoms and commonly discarded by the wine and beverage industries, features high porosity, unique pores, structures and thermal stability, making it an ideal solid support or host for nanocomposite development[21,22] compared to others. Natural diatomite is a safe ingredient to be introduced into medicines and cosmetics[23].

Silver-loaded natural diatomite pores were prepared using electrochemical and thermal calcination methods to promote their use and applicability as nanoparticle carriers[15]. The deposition of silver nanoparticles onto diatomite was confirmed by a visible color change to grey upon completion of the electrochemical process. Subsequently, Ag-diatomite was calcined at temperatures of 300, 500, and 800 ºC yielding the nanoparticles with a size of 50-90 nm. Among obtained materials, silver nanoparticles-diatomite calcined at 300 ºC showed the most effective antibacterial properties against both *Escherichia coli* and *Staphylococcus aureus*. In addition, Ag/GO/diatomite also created as an antibacterial agent[24]. Ag/GO/diatomite calcined at 500 ºC for 4 hours showed that AgNp/GO/diatomite had a better ability to inhibit *E. coli* than *S. aureus*. Furthermore, the AgNPs have been produced on bio-silica diatomite using Pinus Koraiensis extract, resulting in nanoparticle sizes of 27 nm and dispersed homogeneously on the surface of the diatomite[25]. The material exhibited significant antibacterial properties against *E. coli* and *S. aureus*, as evidenced by its capacity to inhibit bacterial growth within 1 hour of contact. Lastly, a silver nanoparticle-natural diatomite with Lantana camara leaf extract yielding a silver nanoparticles with a size range between 20 and 90 nm has been synthesized successfully[26].

In this research, silver-diatomite nanocomposites were synthesized through a green, one-pot method employing pineapple leaf extract as a biogenic reducer and stabilizer. By integrating agricultural biomass, pineapple leaves, and industrial mineral waste, diatomite, the proposed approach not only provides a sustainable route to antibacterial material synthesis but also supports circular economy strategies through waste valorization. The one-pot synthesis approach employed in this study offers several advantages by combining the reducing power of organic phytochemicals with the structural stability of an inorganic support (diatomite). This method simplifies the synthesis process, eliminates the need for external reducing or capping agents, and reduces both reaction time and energy consumption[7]. Furthermore, the simultaneous reduction, stabilization, and deposition of AgNPs onto the diatomite surface in a single step ensures better nanoparticle dispersion and minimizes agglomeration[10]. Compared to conventional multi-step methods, this green one-pot strategy is more environmentally friendly, cost-effective, and scalable. Thus, the selected method provides a practical and efficient route for fabricating antibacterial nanocomposites with enhanced stability and performance. The antibacterial efficacy of the resulting nanocomposites was evaluated against *P. aeruginosa* and *S. aureus*, two clinically significant pathogens. Furthermore, a molecular simulation study was conducted in parallel with experimental work to evaluate the adsorption behavior of key phytochemicals from pineapple leaf extract on the silver (Ag(100)) surface. The uniqueness and highlight of this study its rooted in its integrated approach that combines waste valorization, green nanotechnology, and computational modeling to develop efficient and sustainable antibacterial agents for environmental and biomedical applications.

2. Materials and Method

2.1. Materials

Pineapple leaves were collected from the pineapple plantation area in Jipeng Area, Taichung, Taiwan. $AgNO_3$ was purchased from Sigma–Aldrich, NaOH (Merck) and natural diatomite waste used in this study was obtained from Imerys Filtration Minerals Inc. (Cellite® 577; density = 0.47 g/cm³; composition: 80–90% SiO_2, 2–4% Al_2O_3, and 0.5–2% Fe_2O_3). This diatomite represents a post-consumer industrial waste material, as it had been previously utilized in the wine filtration industry and was repurposed in this work as a porous inorganic support for nanoparticle incorporation.

2.2. Methods

2.2.1. Preparation of Pineapple Leaf (PL) Extract

Pineapple leaves were chopped and dried in the oven at 25-30 ºC for 5 days. A total of 2.5 g of dried leaves was

Cite: S. Kamali et al., "Eco-Engineered Silver-Diatomite Nanocomposites from Agro-Industrial Waste for Sustainable Antibacterial Agent: A Combined Laboratory and Molecular Simulation Study". Evergreen, 12 (04) 1946-1960 (2025). https://doi.org/10.5109/7402627.

extracted using 100 mL of distilled water. The mixture was heated at 60-80 ºC for 1 hour and then filtered. The filtrate was used for one-pot synthesis of AgNp-NDs-PL.

2.2.2. Preparation of Natural Diatomite Waste

The natural diatomite waste from the wine industry was washed with distilled water and acetone to dissolve the polar and organic waste, then calcined at a temperature of 300 ºC for 3h. The sample was then analyzed by TGA analysis.

2.2.3. One-pot Synthesis of Silver Nanoparticles-Natural Diatomite Composites by Pineapple Leaf Extract (AgNp-NDs-PL)

A total of 100 mL of a solution containing 1%, 3%, and 5 % w/w of $AgNO_3$ was mixed with 2.5 mL of PL extract. After 2 hours of heating the solution to 70 ºC, the colour change was observed. Each solution then received the addition of 1 g of diatomite. The mixture was stirred for 24 hours at room temperature to complete the insertion of silver nanoparticles into natural diatomite pores and surfaces. The mixture was then dried at 60 ºC for 48 h to remove the water content, resulting in AgNp-1%-NDs-PL, AgNp-3%-NDs-PL, and AgNp-NDs-5%-PL in a powder form. After performing FTIR, XRD, and SEM-EDX analyses, the sample's antibacterial capabilities were evaluated against *S. aureus* and *P. aeruginosa*.

2.2.4. One-pot synthesis of Silver Nanoparticles-Natural Diatomites by Adsorption and Calcination Methods (AgNp-NDs-Calc)

An amount of 1 g of natural diatomites was added to 1 %, 3%, and 5 % w/w of the $AgNO_3$ solution in which each of the solutions was added with 10 mL of NaOH 1 M. The mixture was stirred for 24 hours to ensure the complete insertion of Ag^+ ions into the pores and surface of the natural diatomite. The water content was removed by heating the mixture at 60 ºC for 48 h. The formation of nanoparticles was observed after the calcination process at 500 ºC for 3 h, resulting in AgNp-1%-NDs-Calc, AgNp-3%-NDs-Calc, and AgNp-5%-NDs-Calc. The composites were analyzed with FTIR spectroscopy, XRD, SEM-EDX, TEM and tested for antibacterial properties against *P. aeruginosa* and *S. aureus*.

2.2.5. Qualitative Antibacterial Assay for AgNp-NDs-PL and AgNp-NDs-Calc against *P. aeruginosa* and *S. aureus*

The potency of AgNp-NDs-PL and AgNp-NDs-Calc as antibacterial agents against *P. aeruginosa* and *S. aureus* was determined using the dilution method. Mueller-Hinton Broth (MHB) was used to cultivate strains of *P. aeruginosa* and *S. aureus*. The preparation of MHB involved dissolving 21 g of MHB in 1000 mL of distilled water. *P. aeruginosa* and *S. aureus* were incubated at 37 °C for 24 h in a biochemical incubator. A total of 50 µL of *P. aeruginosa* or S. aureus bacteria, with 1×10^8 CFU/mL, was incubated in a tube after mixing 4950 µL of MHB medium, then 0.2 g of AgNp-1%-NDs-PL, AgNp-3%-NDs-PL, AgNp-5%-NDs-PL, AgNp-1%-NDs-Calc, AgNp-3%-NDs-Calc, and AgNp-5%-NDs-Calc were added to 5 mL of MHB medium with bacteria in each case. The condition for the antibacterial assay is shown in Table 1. The antibacterial activity was observed from the clarity or turbidity of the solution since it promotes the excellent inhibition of the nanocomposites to bacteria. The clarity of the sample was observed for 24 hours.

Table 1: The antibacterial test for AgNp-NDs-PL (A) and AgNp-NDs-Calc (B) toward *P. aeruginosa* and *S. aureus*

No.	Bacteria	Nanocomposite		Sample name
		A Conc. (wt%)	B Conc. (wt%)	
1.	P. aeruginosa	1		P-1
		3		P-2
		5		P-3
			1	P-4
			3	P-5
			5	P-6
		-	-	Control
2.	S. aureus	1		S-1
		3		S-2
		5		S-3
			1	S-4
			3	S-5
			5	S-6
		-	-	Control

2.2.6. Molecular Simulation of Bioactive Phytochemical Compounds from Pineapple Leaf Extract on Silver Nanoparticles Ag(100) Surfaces

Molecular simulations were performed using the Material Studio 7.0 (Accelrys Inc., San Diego, CA, USA)[27]. The Ag(100) surface was modeled using a periodic slab consisting of a 4 × 4 × 3 supercell with a vacuum layer of 15 Å along the z-axis to prevent interlayer interactions. The COMPASS II force field was used for energy minimization and molecular dynamics simulations. Geometry optimization was carried out using the Smart Minimizer algorithm until the energy convergence reached 1.0×10^{-4} kcal/mol. The cut-off distance for van der Waals and electrostatic interactions was set at 15.5 Å.

Five major phytochemical constituents in pineapple leaf extract such us, 1-O-caffeoylglycerol, 1-O-coumaroylglycerol, p-coumaric acid, and 1,3-O-dicaffeoylglycerol, and caffeic acid were selected. The selection of phenolic compounds used in the molecular simulation was based on reported literature describing the major bioactive constituents present in pineapple leaf extract[28]. The molecular structures of each compound

were first optimized using the Forcite module with the COMPASS force field. A silver slab with a (100) surface orientation was constructed and relaxed to serve as the adsorption substrate. Each optimized molecule was then docked onto the Ag(100) surface, and a full geometry optimization was conducted to determine the most stable configuration. The adsorption energy (E_{ads}) was calculated using the equation:

$$\boldsymbol{E_{ads} = E_{total} - (E_{surface} + E_{molecule})} \quad (1)$$

Where:
E_{ads} is the adsorption energy,
E_{total} is the energy of the surface-adsorbate system,
$E_{surface}$ is the energy of clean Ag(100) surface, and
$E_{molecule}$ is the energy of the isolated molecule in vacuum.

3. Result and Discussion

3.1. TGA analysis of natural diatomite waste

Thermal analysis of natural diatomite waste was carried to determine the successful removal of impurities/organic matter during the calcination process at 300 °C for 3 hours. The primary thermograms for natural diatomite waste before and after heat treatment is shown in Figure 1. The measured residual materials from the thermal analysis for the natural diatomite waste before and after calcination were 95.31% and 99.23%. The organic compounds in the natural diatomite used resulted from the wine filtration process. At the final analysis temperature (580 °C), 3.92% of the impurities were successfully reduced and removed from the pores and structure of diatomite.

3.2. Green synthesis of AgNp-NDs-PL Nanocomposite using Pineapple Leaf Extract (PL)

The synthesis of AgNp-NDs-PL Nanocomposite was initiated from the synthesis of AgNp by pineapple leaf extract. The successful formation of AgNPs was observed by the changes of the colour of the solution that becoming reddish-brown (Figure 2). The reddish-brown colour is the characteristic colour for AgNp formation obtained after adding leaf extract and after heating process[7].

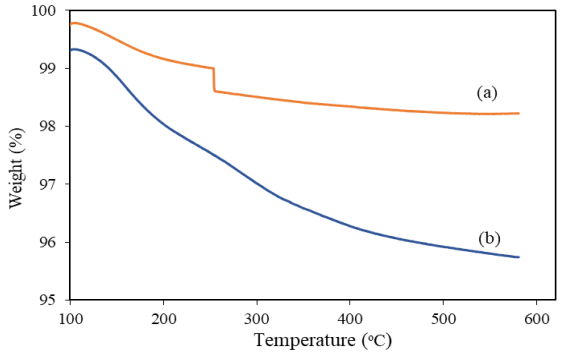

Fig. 1: TGA Thermogram of natural diatomite waste (a) after calcination (b) before calcination

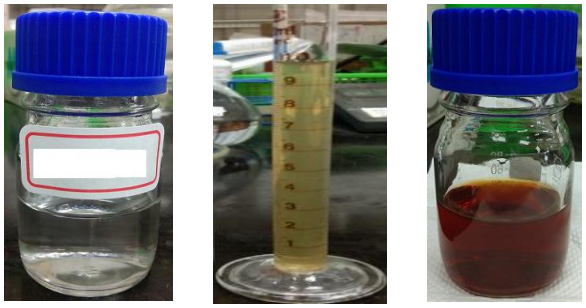

(a) (b) (c)

Fig. 2: The changes of Ag solution colour after the AgNp formation, (a) Ag^+ solution, (b) Pineapple leaf extract, (c) AgNp solution

The color of the solution changed as a result of the reduction of Ag^+ to Ag^0 nanoparticles. This reduction occurred due to the reaction between phytochemical compounds in pineapple leaf extract and Ag^+ ions in solution. The phytochemicals serve as electron donors to the metal orbitals, facilitating the reduction process. Their high electron density enables them to function as capping agents, thereby stabilizing and maintaining the size of the resulting nanoparticles[5,29]. The formation of Ag nanoparticles was observed by Particle Size Analysis, (Figure 3).

Figure 3 illustrates the particle size distribution profiles of silver–diatomite nanocomposites synthesized using varying concentrations of $AgNO_3$. The legend in this Figure refers to the following three sample formulations, samples (a) AgNp-1%-NDs-PL, (b) AgNp-3%-NDs-PL, and (c) AgNp-5%-NDs-PL exhibited average particle sizes (D50) of approximately 27 nm, 45 nm, and 65 nm, respectively. The size distributions ranged from 1 to 100 nm, depending on the synthesis route and stabilization conditions. These results demonstrate that the green one-pot synthesis method enables effective control over nanoparticle size, with the smallest and most uniform particles obtained in the AgNp-1%-NDs-PL sample. The observed differences may be attributed to variations in extract concentration, and silver nanoparticle loading.

The gravimetric technique also demonstrated the successful insertion of silver nanoparticles into diatomite pores (Table 2). The number of silver nanoparticles loaded to natural diatomites was 1.29, 3.21, and 5.19 %w/w, in line with the initial loaded concentration of Ag^+, which was 1, 3, and 5 %w/w. A slight difference in weight percentage was observed between Ag^+ initial and AgNp-NDs-PL because of the existence of the phytochemicals compound from pineapple leaf extract as shown in Figure 4. The white powder, as an intrinsic colour of natural diatomite (a), became a brownish colour (b, c, d), indicating that the AgNps already loaded into natural diatomite pores and structures. One limitation of using diatomite as a support material is its lack of organic functional groups, which are essential for stabilizing nanoparticles during synthesis. These functional groups

Cite: S. Kamali et al., "Eco-Engineered Silver-Diatomite Nanocomposites from Agro-Industrial Waste for Sustainable Antibacterial Agent: A Combined Laboratory and Molecular Simulation Study". Evergreen, 12 (04) 1946-1960 (2025). https://doi.org/10.5109/7402627.

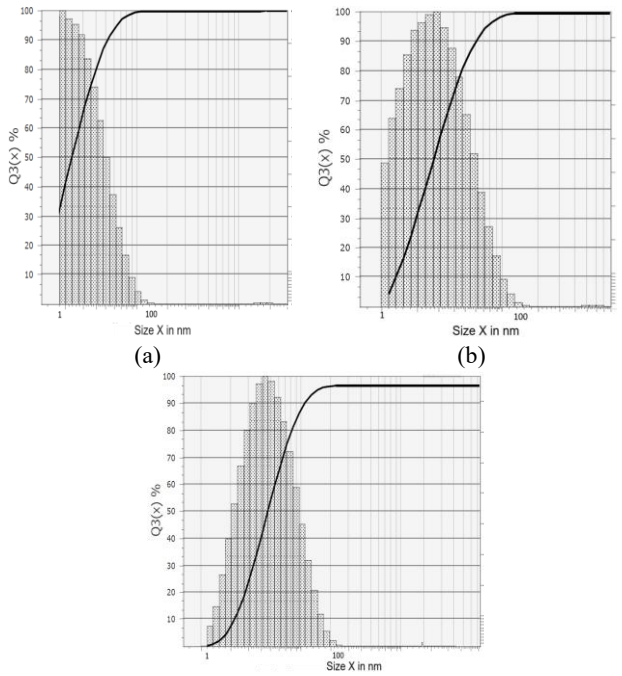

Fig. 3: The Particle sizes observation of (a) AgNp-1%-NDs-PL, (b) AgNp-3%-NDs-PL, and (c) AgNp-5%-NDs-PL

Table 2: The percentage of silver nanoparticles loaded on AgNp-1%-NDs-PL (1), AgNp-3%-NDs-PL (2), and AgNp-5%-NDs-PL (3) pores and structure

No.	W_o* (g)	W_f*(g)	Amount of AgNp Loaded (*wt*%)
1.	1.007±0.002	1.020 ± 0.003	1.29 ± 0.04
2.	1.004±0.001	1.036 ± 0.002	3.21 ± 0.07
3.	1.008±0.003	1.060 ± 0.003	5.19 ± 0.06

**W_o = initial weight of natural diatomite, W_f* = final weight of AgNp-NDs-PL (data are presented as mean ± standard deviation (n = 3).*

act as capping agents that help maintain nanoparticle size in colloidal form. After the drying process, however, nanoparticles become susceptible to agglomeration in the absence of such stabilizers. Nevertheless, the high surface area and porous structure of diatomite contribute to preserving the nanoscale size of the particles in powder form after separation from the bio-reductant. The combination of diatomite with organic compounds, such as phytochemicals from plant extracts, offers a synergistic effect that maintains nanoparticle stability in both solution and solid states.

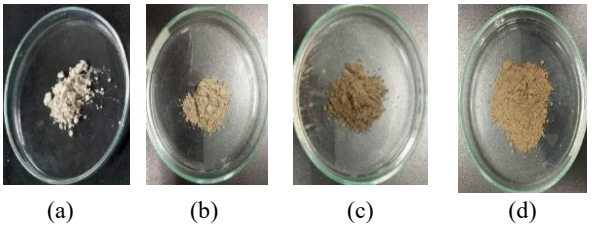

Fig. 4: The digital image of (a) natural diatomite and AgNp-NDs-PL in different concentrations of (b) AgNp-1%-NDs-PL, (c) AgNp-3%-NDs-PL, (d) AgNp-5%-NDs-PL

3.3. Green synthesis of AgNp-NDs-Calc Nanocomposite with calcination method

The synthesis of AgNp-NDs-Calc began with the entrapment of Ag^+ on natural diatomite pores and surfaces. The addition of sodium hydroxide to the Ag^+NDs mixture changed the natural diatomite colour becoming grey as a result of the formation of AgOH species in the solution, an unstable species that easily forms black precipitate of Ag_2O. Furthermore, the grey indicated that not all the $AgNO_3$ in the mixture decomposed to Ag_2O, where some of Ag species remained in the Ag^+NDs form. The illustration of the nanoparticle reduction process is shown in Figure 5. The formation of Ag_2O on the natural diatomite surface resulted in an easy way to synthesize nanoparticles by the calcination process at high temperatures. The heat process forces the reduction of silver to nanoparticles form (Ag_2O--(Si-O)n to Ag^0--(Si-O)n). At high temperatures, the intermolecular silver bond weakens and tends to reorganize itself into the silica network of the diatomite structure. A high temperature not only affects the metal bond but also reduces the molecular sizes of diatomite. High heat exposure during the calcination process reduces the diatomite pore size to the nanoscale range of 50–100 nm, although some pores remain with sizes below 4000 nm[30], making it a possible template for the formation of nanoparticles. Diatomite acts as a filler and host for the rearrangement of metal structures to nano-size structures[16,17,25]. The calcination process reduces the metal and has a higher potential effect on nanoparticle formation. The appearance of AgNp-NDs-Calc in different concentrations is shown in Figure 6. The darker color of the AgNp-NDs-Calc nanocomposite, as compared to AgNp-NDs-PL (Figure 4), is due to the incomplete reduction of Ag2O--(Si-O)n species to Ag0--(Si-O)n. As a result, some Ag2O remains on the natural diatomite surface.

The gravimetric analysis also indicated the silver nanoparticle supported on diatomite structure. The

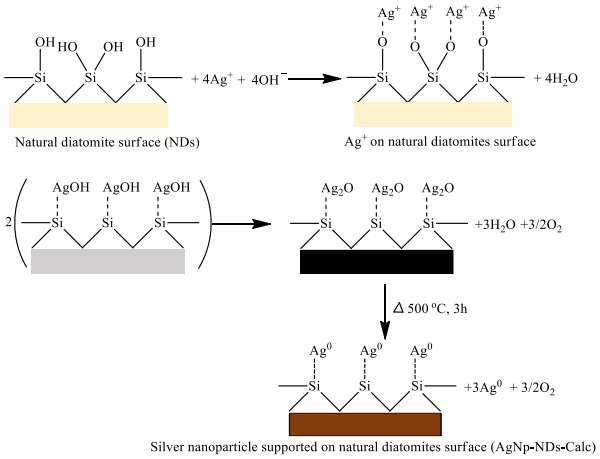

Fig. 5: The reaction of the calcination process to produce silver nanoparticles-diatomite (AgNp-NDs-Calc) in NaOH addition

Fig. 6: The AgNp-NDs-Calc with different AgNp percentage, (a) AgNp-1%-NDs-Calc, (b) AgNp-3%-NDs-Calc and (c) AgNp-5%-NDs-Calc after calcination process at a temperature of 500 °C for 3 h

Table 3: The percentage of AgNp supported on AgNp-1%-NDs-Calc (1), AgNp-3%-NDs-Calc (2) and AgNp-5%-NDs-Calc (3) structure

No.	W_o* (g)	W_f*(g)	The amount of AgNp Loaded (*wt*%)
1.	1.001 ± 0.002	1.011 ± 0.002	1.01 ± 0.03
2.	1.005 ± 0.001	1.035 ± 0.001	3.00 ± 0.05
			The amount of AgNp/Ag_2O Loaded (*wt*%)
3.	1.008 ± 0.002	1.058 ± 0.003	5.03 ± 0.04

**W_o = initial weight of natural diatomite, W_f* = final weight of AgNp-NDs-Calc (data are presented as mean ± standard deviation (n = 3).*

technique calculated the number of silver nanoparticles successfully supported on natural diatomite pores, and the structure is summarized in Table 3.

3.4. The X-Ray Diffractometer (XRD) Analysis

3.4.1. XRD Analysis of AgNp-NDs-PL

The successful insertion of silver nanoparticles into natural diatomites was confirmed by the presence of characteristic peaks (Figure 7). The peaks at 2θ=20.24, 27.36, and 34.17° were confirmed as characteristic peaks for silicate compounds as the primary composition of natural diatomite[23]. The characteristic peaks corresponding to the silver nanoparticles for the face centered cubic crystalline structure at 2θ=37.43, 44.17, 64.39, 77.61, and 81.73° are shown in Table 4. The peaks 4 and 5 in AgNp-1%-NDs-PL (b) are very weak because concentration of AgNp in the natural diatomite's structure was very low. The existence of AgNp on AgNp-1%-NDs-PL structure was observed by the EDX spectra on Figure 14.

The successful insertion of silver nanoparticles into natural diatomites was confirmed by the presence of characteristic peaks (Figure 7). The peaks at 2θ=20.24, 27.36, and 34.17° were confirmed as characteristic peaks for silicate compounds as the primary composition of natural diatomite[23]. The characteristic peaks corresponding to the silver nanoparticles for the face centered cubic crystalline structure at 2θ=37.43, 44.17, 64.39, 77.61, and 81.73° are shown in Table 4. Based on the Scherrer formulation, the crystallin size of AgNps was 17.56 nm[31]. The peaks 4 and 5 in AgNp-1%-NDs-PL (b) are very weak because

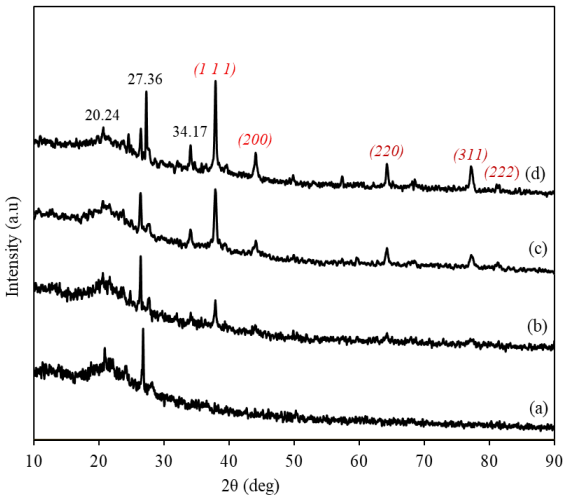

Fig. 7: XRD diffractograms of (a) natural diatomites, (b) AgNp-1%-NDs-PL, (c) AgNp-3%-NDs-PL, and (d) AgNp-5%-NDs-PL nanocomposites

concentration of AgNp in the natural diatomite's structure was very low. The presence of Ag nanoparticles in the AgNp-1%-NDs-PL sample was confirmed by the EDX spectrum shown in Figure 14.

3.4.2. X-Ray Diffraction of AgNp-NDs-Calc

The characteristic peaks of various concentrations of AgNp-NDs-Calc are shown at 2θ= 37.90, 44.20, 64.38, 77.48, 81.56° which confirmed that silver nanoparticles succeeded in supporting on the natural diatomite structures by the calcination methods (Figure 8). The peak at 2θ=31.34° corresponds to Ag_2O-NPs formation[32], indicated by the darker color of AgNp-NDs-Calc (Figure 6). The calcination process at 500°C resulted in growing nanoparticles on the natural diatomite pore and surface[16]. Based on the XRD analysis, a diffraction peak at 2θ = 31.34° (110) was observed specifically in the AgNp-5%-NDs-Calc sample. This peak corresponds to the (111) plane of silver oxide (Ag_2O) (JCPDS No. 41-1104), indicating that a portion of silver in this sample exists in the oxidized state. In contrast, the main diffraction peaks associated with metallic Ag^0-NP were consistently observed at 2θ ≈ 37.90°, 44.2°, 64.38°, 77.48° and 81.56° (JCPDS No. 04-0783) in all samples. Therefore, the total silver content of 5.03% in the AgNp-5%-NDs-Calc sample (as reported in Table 3) includes both metallic Ag^0-NP and Ag_2O-NP.

3.5. Porous Structure of Diatomite, AgNp-NDs-PL and AgNp-NDs-Calc nanocomposite

The SEM analysis results exhibited the existence of AgNps on the natural diatomite surfaces and pores. The particle sizes of AgNp-NDs-Calc are bigger than those of AgNp-NDs-PL. The AgNp-NDs-Calc average size was 70.40 nm[7]. The calcination process at 500 °C was successful to control the particle size and stability of nanoparticles,

Cite: S. Kamali et al., "Eco-Engineered Silver-Diatomite Nanocomposites from Agro-Industrial Waste for Sustainable Antibacterial Agent: A Combined Laboratory and Molecular Simulation Study". Evergreen, 12 (04) 1946-1960 (2025). https://doi.org/10.5109/7402627.

Table 4: The 2θ characteristics peaks for AgNp-NDs-PL and AgNp-NDs-Calc nanocomposites

AgNp-NDs-PL			AgNp-NDs-Calc		
Peak No.	2θ (°)	hkl	Peak No.	2θ (°)	hkl
1.	37.43	(111)	1.	31.34	(110)
2.	44.17	(200)	2.	37.90	(111)
3.	64.39	(220)	3.	44.20	(200)
4.	77.61	(311)	4.	64.38	(220)
5.	81.73	(222)	5.	77.48	(311)
			6.	81.56	(222)

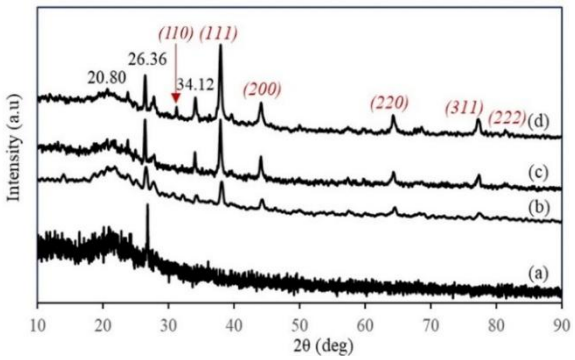

Fig. 8: The X-ray diffractograms of (a) natural diatomite, (b) AgNp-1%-NDs-Calc, (c) AgNp-3%-NDs-Calc, and (d) AgNp-5%-NDs-Calc

while the hydrothermal process by using the plant extract resulted the smallest sizes of nanoparticle. The porous structure of diatomite, AgNp-NDs-PL and AgNp-NDs-Calc nanocomposites is shown in Figure 9 and Figure 10. Figure 10 presents TEM images of the AgNP-NDs-Calc composites synthesized with varying silver loadings: (a) AgNp-1%-NDs-Calc, (b) AgNp-3%-NDs-Calc, and (c) AgNp-5%-NDs-Calc. All images show silver nanoparticles (dark contrast) successfully deposited on the porous diatomite surface. In sample (a), the nanoparticles are small and well-dispersed, indicating effective stabilization at low silver loading. In sample (b), a moderate increase in particle density is observed, with some degree of particle clustering. Sample (c) shows a noticeably higher concentration of silver nanoparticles with larger particle sizes and occasional agglomeration, likely due to higher precursor concentration and insufficient surface capping. These observations suggest that increasing silver loading leads to a gradual transition from uniform dispersion to localized aggregation, which may influence the material's surface area and antibacterial performance. The red circle in Fiure. 10 highlights the AgNPs located on the surface of diatomite pores.

Although stability testing was not conducted as a separate analysis, the morphological and particle size data PSA (Figure 3) and TEM (Figure 10) suggest that the synthesized AgNP–NDs-PL and AgNP–NDs-Calc nanocomposites-maintained nanoscale dispersion without aggregation. This structural stability is likely due to the synergistic effect of phytochemical capping and diatomite's high surface area and porosity, which effectively anchor the nanoparticles and inhibit agglomeration

3.6. The comparison of antibacterial properties of AgNp-NDs-PL and AgNp-NDs-Calc against *P. Aeruginosa* and *S. Aureus* Bacteria

3.6.1. Antibacterial properties against *P. Aeruginosa* bacteria

P. aeruginosa is a gram-negative bacterium, aerobic-facultatively anaerobic, and particularly found in freshwater. This bacterium causes infections such as folliculitis, osteomyelitis, pneumonia, otitis externa, and many more[33]. The antibacterial test was observed in liquid media because the bacteria are mostly found in freshwater. The antibacterial performance of the material was evaluated based on the turbidity of the bacteria-containing solution. The observation of the turbidity indicates the specific concentration to inhibit the bacterial growth. A less turbid or clear solution indicates effective bacterial inhibition by the sample, as fewer bacterial cells are able to grow and multiply. In contrast, a turbid solution suggests that bacterial growth was not effectively inhibited. Besides, the cloudy solution indicates the low performance or no antibacterial properties of the material. The antibacterial test for AgNp-1%-NDs-PL, AgNp-3%-NDs-PL, AgNp-5%-NDs-PL resulted the clear solution (P1, P2, P3). Meanwhile, the antibacterial test towards AgNp-1%-NDs-Calc depicted a cloudy solution (P4) (Figure 11). In the highest concentration of silver nanoparticles, 3% and 5%, yielded the less turbid solution (P5, P6) that indicated that both methods could be employed as effective way to synthesize silver nanoparticles-diatomite with excellent antibacterial properties. However, the nanocomposite synthesized by pineapple leaf extract (AgNp-NDs-PL) has an excellent antibacterial toward P. aeruginosa in lowest concentration of AgNPs compared with the AgNp-NDs-Calc. The smaller sizes of AgNp-NDs-PL was contributed into the ability of nanoparticles to penetrates into protective outer shell of gram-negative bacteria. These bacteria are generally more harmful than Gram-positive ones due to the additional outer shell, which contributes to antibiotic resistance. Besides, the smaller sizes of AgNp-NDs-PL produce effective contact between nanocomposite and bacteria, affecting the strongest inhibition of bacterial growth. In addition to the size effect, the enhanced antibacterial properties of AgNp-NDs-PL are attributed to the phytochemical compounds present in the pineapple leaf extract, which further strengthen its antibacterial activity. According to Loon et al., 2018, the composition of phenolic compounds in pineapple leaves potentially acts as an antibacterial agent[6]. The FTIR analysis of AgNp-1%-NDs-PL and AgNp-1%-NDs-Calc in Figure 12, shows

the functional group of the phytochemical compound contained in AgNp-1%-NDs-PL.

The AgNPs, stabilized by phenolic compounds (such as 1,3-O-dicaffeoylglycerol), adsorb onto the bacterial cell wall due to electrostatic interactions and the high surface area provided by the porous diatomite matrix. In addition, the phenolic compounds enhance the generation of reactive oxygen species (ROS) through redox cycling of their catechol moieties. These compounds also disrupt the lipid bilayer by interacting with the phospholipid membrane via reactive hydroxyl or catechol groups, leading to increased membrane permeability. The enhanced permeability facilitates the diffusion of ROS into the bacterial cell, resulting in oxidative damage to proteins, lipids, and nucleic acids. Moreover, the increased membrane permeability allows small-sized AgNPs to more readily penetrate the bacterial cytoplasm. Once inside, the AgNPs gradually release Ag^{+} ions, which bind to thiol groups in bacterial enzymes and DNA, thereby interfering with respiration and replication processes. The proposed

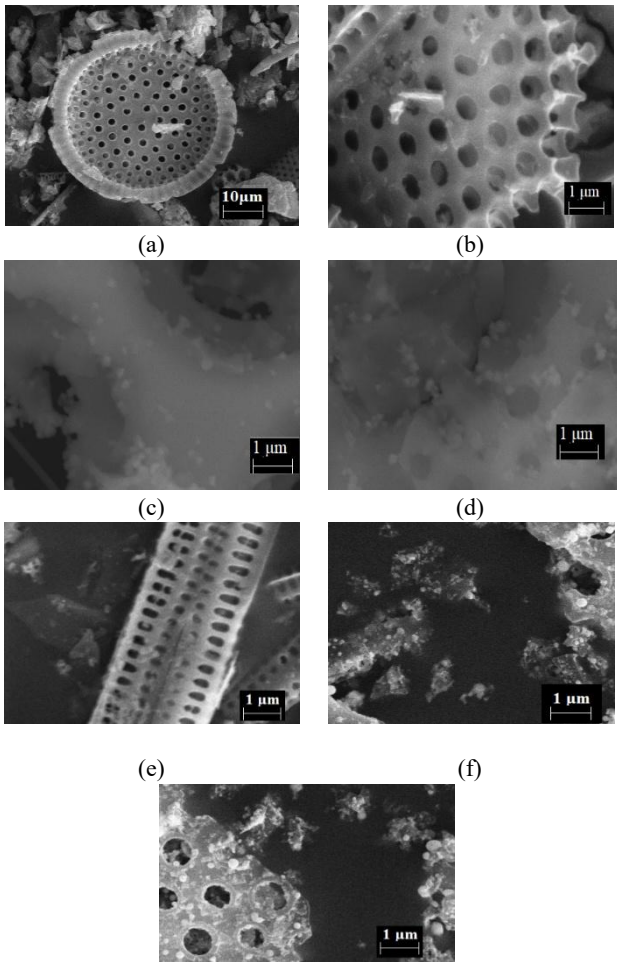

Fig. 9: SEM images of (a) natural diatomite, (b) AgNp-1%-NDs-PL, (c) AgNp-3%-NDs-PL, (d) AgNp-5%-NDs-PL, (e) AgNp-1%-NDs-Calc, (f) AgNp-3%-NDs-Calc, (g) AgNp-5%-NDs-Calc nanocomposites at various magnifications

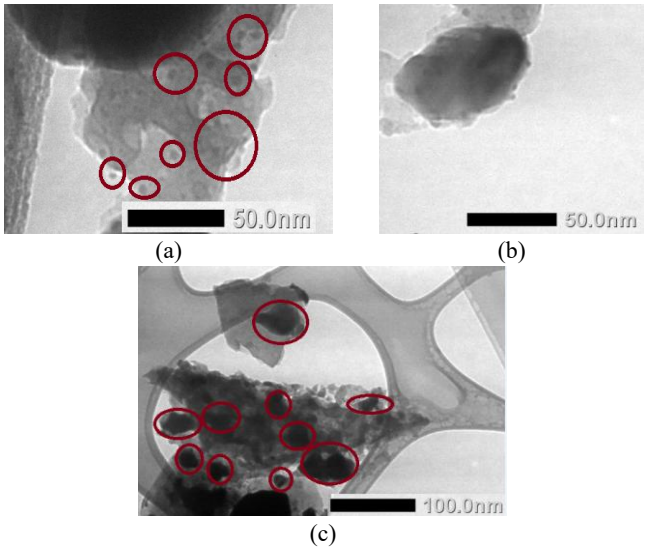

Fig. 10: TEM analysis of (a) AgNp-1%-NDs-Calc, (b) AgNp-3%-NDs-Calc, (c) AgNp-5%-NDs-Calc

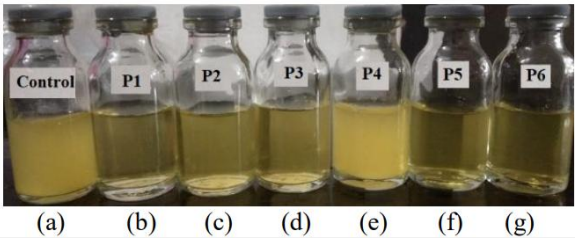

Fig. 11: Antibacterial properties of AgNP-NDs-PL and AgNP-NDs-Calc toward P. Aeruginosa, after 24 h contact (a) Control, (b) P1=AgNp-1%-NDs-PL, (c) P2=AgNp-3%-NDs-PL, (d) P3=AgNp-5%-NDs-PL, (e) P4=AgNp-1%-NDs-Calc, (f) P5=AgNp-3%-NDs-Calc, (g) P6=AgNp-5%-NDs-Calc

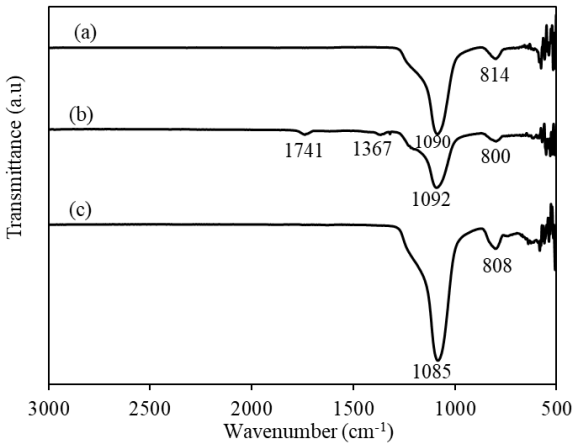

Fig. 12: Infrared spectra of (a) natural diatomite and (b) AgNp-1%-NDs-PL, (c) AgNp-1%-NDs-calc

antibacterial mechanism of the AgNP-NDs-PL nanocomposite is illustrated in Figure 13.

The additional FTIR peaks at 1741 and 1367 cm-1 for AgNp-1%-NDs-PL are correlated to -C=O groups and -C-H stretching from phenolic compounds in pineapple leaf. While FTIR analysis (Figure 12) did not show distinct

Table 5: Elemental composition of natural diatomite and AgNp-1%-NDs-PL determined by EDX analysis

No.	Natural diatomite		Mass (wt%)	AgNp-1%-NDs-PL		Mass (wt%)
	Element	Atomic Number		Element	Atomic Number	
1.	Si	14	55.28	Si	14	46.08
2.	O	8	33.18	O	8	38.10
3.	C	6	9.63	C	6	15.45
4.	Al	13	0.58	Al	13	0.37
5.	-			Ag	47	1.01
6.	-			S	16	0.21
7.	-			P	15	0.20

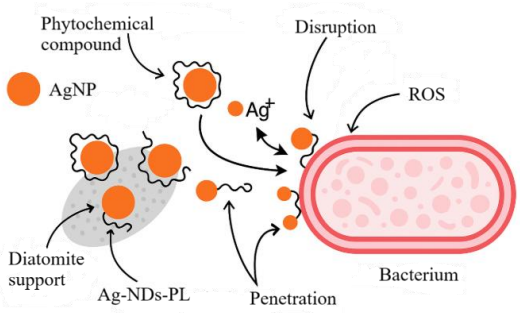

Fig. 13: The proposed antibacterial mechanism of the AgNP-NDs-PL nanocomposite

bands corresponding to phenolic O–H stretching (typically at 3200–3550 cm^{-1}), this may be due to overlapping with broad –OH vibrations from diatomite or adsorbed moisture, or to the low abundance of residual phenolics post-synthesis. The peaks at 1085 and 808 cm^{-1} (c), 1092 and 800 cm^{-1} (b), and 1090 and 814 cm^{-1} (a) were observed as Si-O- asymmetric stretching vibration of siloxane groups (Si-O-Si) from natural diatomite structure. The composition AgNp-1%-NDs-PL was observed from the EDX spectra shown in Figure 14 and Table 5.

Table 5 presents the elemental composition of natural diatomite and AgNp-1%-NDs-PL, highlighting the composition changes that occurred after silver nanoparticle deposition using pineapple leaf extract. The silicon (Si) content decreased from 55.28 wt% in natural diatomite to 46.08 wt% in the composite, indicating partial surface coverage by silver nanoparticles and organic compounds, which likely masked the silicate signal during EDX analysis. Conversely, the oxygen (O) content increased from 33.18 wt% to 38.10 wt%, attributed to the presence of silver oxides and oxygenated functional groups from phytochemicals in the pineapple leaf extract. A significant increase in carbon (C) content, from 9.63 wt% to 15.45 wt%, confirmed the incorporation of phytochemical compounds, which serve as both reducing and capping agents during synthesis and remain attached to the nanocomposite surface. The appearance of silver (Ag) at 1.01 wt% in the composite, which was absent in natural diatomite, confirms successful AgNP deposition. Additionally, phosphorus (P) and sulfur (S) were detected only in the AgNp-1%-NDs-PL sample at 0.20 wt% and 0.21 wt%, respectively, suggesting their origin from trace elements or residual compounds in the leaf extract. The EDX data confirm the successful functionalization of diatomite with silver nanoparticles synthesized using pineapple leaf extract, which contribute to the improved antibacterial properties of the composite.

3.6.2. Antibacterial Properties Towards *S. aureus*

S. aureus were gram-positive bacteria that has a thicker peptidoglycan layer than that of gram-negative bacteria P. aeruginosa[34,35]. The thicker walls make it difficult for silver nanoparticles to enter the bacterial membranes. The antibacterial test for nanocomposite AgNp-NDs-PL and AgNp-NDs-Calc is shown in Figure 15. The test found that AgNp-5%NDs-Calc ultimately inhibited the *S. aureus* bacterial growth after 24 hours of contact, as indicated by the clear solution formation (S6). Meanwhile, the AgNp-NDs-PL showed bacterial growth inhibition in the lower concentration of silver nanoparticles. The AgNp-3%-NDs-PL and AgNp-5%-NDs-PL showed excellent antibacterial properties by the formation of a clear solution (S2, S3). The material synthesized using pineapple leaf extract showed a strong antibacterial effect against S. aureus even at a lower AgNP concentration starting from 3 w/w%. In contrast, the material synthesized via the calcination method exhibited significant inhibition starting at 5 w/w % AgNP concentration.

A comparative analysis was carried out with previously reported Ag-diatomite-based materials. Table 6 summarizes the antibacterial indicators, target microorganisms, synthesis methods, and relative inhibition performance. The table highlights the effectiveness of green-synthesized AgNp-NDs-PL and AgNp-NDs-Calc composites in comparison with other Ag-diatomite materials reported in the literature. This comparison provides a broader perspective on the potential of waste-derived nanocomposites, particularly those incorporating pineapple leaf extract, as sustainable and efficient antibacterial agents against both Gram-positive (*S. aureus*) and Gram-negative (*E. coli*, *P. aeruginosa*) bacteria.

Table 6: Comparative Antibacterial Performance of Various Ag-Diatomite-Based Nanocomposites Against Gram-Positive and Gram-Negative Bacteria

Material	Antibacteria Indicator	Micro organisms Tested	Synthesis Method	Relative Performance
AgNp-NDs-1%-PL (This study)	Clear/ less turbid broth	P. aeuriginosa	Green synthesis using pineapple leaf extract + diatomite	Strong inhibition
AgNp-NDs-3%-PL (This study)	Clear/ less turbid broth	S. aureus		Strong inhibition
AgNp-NDs-3%-Calc. (This study)	Clear/ less turbid broth	P. aeuriginosa	Calcination method	Strong inhibition
AgNp-NDs-5%-Calc. (This study)	Clear/ less turbid broth	S. aureus	Calcination method	Strong inhibition
AgNP-NDs (300ºC calcination process)[16]	slightly turbid	S. aureus, E. coli	Electro-lytic cell, which cathode and anode are Ti and Ag	Moderate inhibition
AgNP/GO/Diatomite[25]	Clear/ less turbid broth	E. coli	Chemical reaction with $NaBH_4$	Strong inhibition
	slightly turbid	S. aureus		Moderate inhibition
4.70%Ag/6.31%Ce/Diatomite[36]	Clear/ less turbid broth	S. aureus	Reducing agent CeO_2	Strong inhibition
2.26%Ag/2.52%Ce/Diatomite[36]	slightly turbid	E. coli		Moderate inhibition

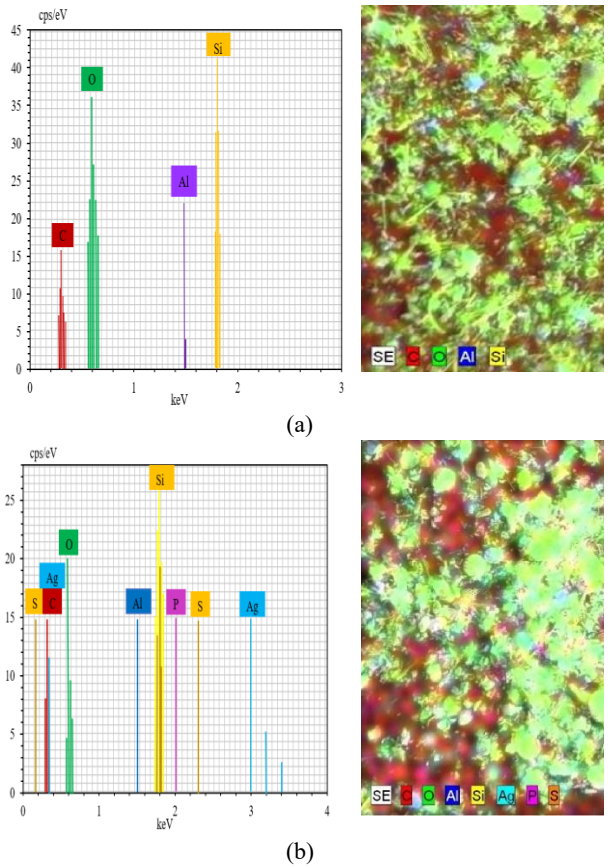

(a)

(b)

Fig. 14: EDX spectra of (a) natural diatomite, and (b) AgNp-1%-NDs-PL

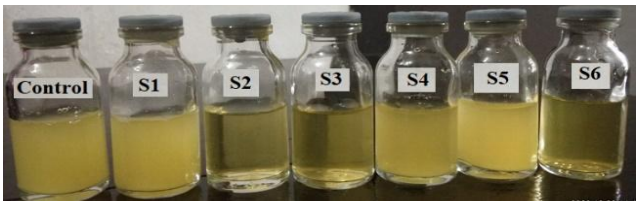

(a) (b) (c) (d) (e) (f) (g)

Fig. 15: Antibacterial properties of AgNp-NDs-PL and AgNp-NDs-Calc toward S. Aureus, after 24 h contact (a) Control, (b) S1=AgNp-1%-NDs-PL, (c) S2=AgNp-3%-NDs-PL, (d) S3=AgNp-5%-NDs-PL, (e) S4=AgNp-1%-NDs-Calc, (f) S5=AgNP-3%-NDs-Calc, (g) S6=AgNp-5%-NDs-Calc

3.7. Molecular simulation for phytochemical compounds from pineapple leaf extract on the silver (Ag(100)) surface

To elucidate the interaction mechanisms between bioactive compounds and the silver nanoparticle surface, molecular simulations were performed using Materials Studio 7.0 with the COMPASS force field. This simulation focused on five major phytochemical constituents identified in pineapple leaf extract: 1-O-caffeoylglycerol, 1-O-coumaroylglycerol, p-coumaric acid, 1,3-O-dicaffeoylglycerol, and caffeic acid. Each molecule was subjected to geometry optimization to reach a stable energy conformation, followed by adsorption studies onto a modeled silver (Ag(100)) surface slab. The adsorption energies were calculated using equation 1.

The adsorption energy data of various phenolic compounds on the Ag(100) surface reveals significant insights into their interaction strength and potential for

surface functionalization. Among the individual compounds, 1,3-O-dicaffeoylglycerol exhibited the highest adsorption energy (-151.268 kJ/mol), indicating robust interaction with the silver surface, likely due to its multiple hydroxyl and aromatic groups, which facilitate multiple contact points via π–π stacking and hydrogen bonding (Table 7 and Figure 16). This can be attributed to the presence of multiple caffeoyl groups that offer numerous active sites for bonding, thereby enhancing the overall interaction. Other compounds such as 1-O-coumaroylglycerol (-86.106 kJ/mol) and 1-O-caffeoylglycerol (-82.574 kJ/mol) also showed relatively strong adsorption, likely due to the glycerol moiety providing additional hydroxyl groups that facilitate binding. In contrast, simpler phenolic acids like caffeic acid (-69.525 kJ/mol) and p-coumaric acid (-65.493 kJ/mol) exhibited moderate adsorption, possibly due to their limited number of interactive functional groups.

Notably, the combination of all five molecules yielded a highly negative adsorption energy of -478.613 kJ/mol, suggesting a synergistic effect that significantly enhances the binding affinity to the Ag(100) surface. This synergism could be due to cooperative interactions among the molecules or increased surface coverage. The cooperative interactions among diverse phytochemicals may promote a denser, more stable organic layer on the silver surface. Such synergy can increase the protective and functionalizing capabilities of the phytochemicals, thereby enhancing the antibacterial activity and nanoparticle stability.

Recent studies support these findings. For instance, Baran *et al.* demonstrated that silver nanoparticles synthesized using *Ananas comosus* fruit peels exhibit significant antimicrobial activities, attributing this to the rich phenolic content of the extracts[37]. Similarly, Hashib *et al.* reported the successful synthesis of silver nanoparticles using pineapple peel extract, highlighting the role of phenolic compounds as reducing and capping agents[38]. These studies underscore the potential of natural phenolic mixtures, such as those derived from pineapple extracts, in stabilizing silver surfaces for applications like antimicrobial coatings, antioxidant films, or environmentally friendly nanomaterials. This combined approach enabled the identification of 1,3-O-dicaffeoylglycerol as the compound with the strongest interaction with the silver surface, suggesting it plays a dominant role in enhancing the antibacterial performance of the nanocomposite.

The molecular simulation insights corroborate the experimental findings where AgNp-NDs-PL, synthesized via pineapple leaf extract, exhibited superior antibacterial activity against Pseudomonas aeruginosa, even at lower concentrations of silver nanoparticles compared to the AgNp-NDs-Calc nanocomposite. The strong interactions modeled in silico help to rationalize the enhanced efficacy,

Table 7: Adsorption Energies of Phytochemical compound in pineapple leaf extract on (Ag(100)) surface based on Computational Simulation

Compound	Adsorption Energy (kJ/mol)
1-O-caffeoylglycerol	-82.574
1-O-coumaroylglycerol	-86.106
p-coumaric acid	-65.493
1,3-O-dicaffeoylglycerol	-151.268
Caffeic acid	-69.525
Combination	-478.613

as phytochemicals not only act as reducers and stabilizers during synthesis but remain bound to the AgNP surface, conferring bioactive functional properties. This enhanced activity is attributed to the presence of residual phytochemical compounds in the AgNp-NDs-PL, which synergistically strengthen its antibacterial effect. This is consistent with the results of simulation studies, which showed that 1,3-O-dicaffeoylglycerol can significantly enhance the antibacterial performance of diatomite-based materials.

Furthermore, the visualization of side and top views (Figure 16) illustrates that the molecules adopt flat orientations on the Ag(100) surface, maximizing contact area. This spatial arrangement supports efficient electron transfer and interfacial stability, which are critical in antimicrobial mechanisms particularly in the generation of reactive oxygen species and membrane disruption in bacteria.

Based on molecular simulation data, 1,3-O-dicaffeoylglycerol is proposed as the dominant compound responsible for reducing Ag^{+} to Ag^{0} in the green synthesis route. This molecule contains two caffeic acid moieties, each of which possesses a catechol group (i.e., an ortho-dihydroxybenzene ring) esterified at the 1 and 3 positions of the glycerol backbone. During the reduction of Ag^{+} to Ag^{0}, the catechol groups in each caffeoyl unit can donate electrons and become oxidized to quinone structures. The resulting oxidized molecule is commonly referred to as a quinonoid intermediate. This intermediate subsequently acts as a capping and stabilizing agent in the formation of silver nanoparticles (AgNPs). An illustration of AgNP formation mediated by 1,3-O-dicaffeoylglycerol is provided in Figure 17.

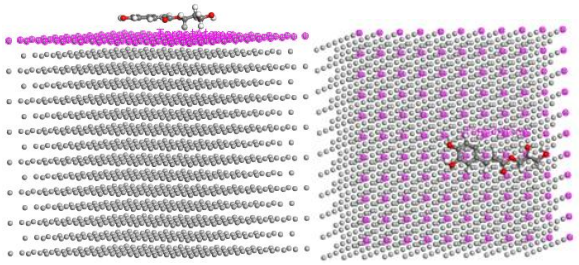

(a)

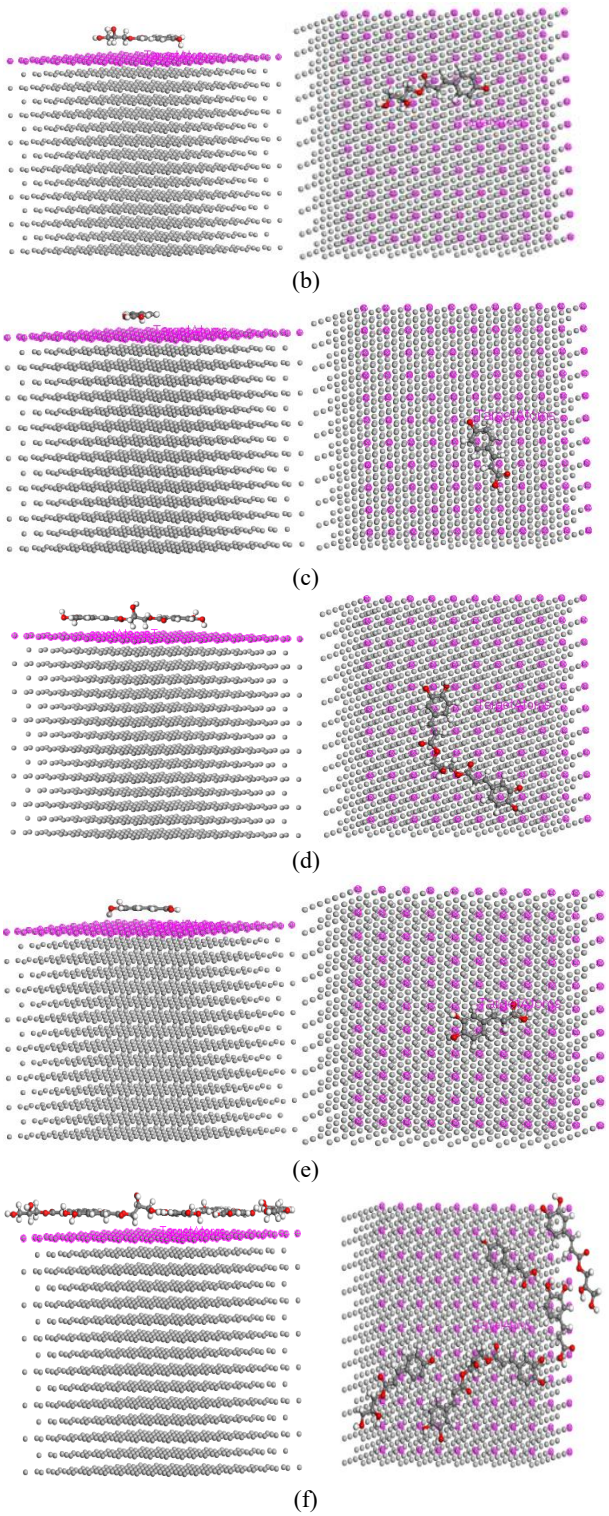

Fig. 16: Side and top view interaction of (a) 1-O-caffeoylglycerol, (b) 1-O-coumaroylglycerol, (c) *p*-coumaric acid, (d) 1,3-O-dicaffeoylglycerol, (e) Caffeic acid, (f) Compound Combination on the silver (Ag(100)) surface

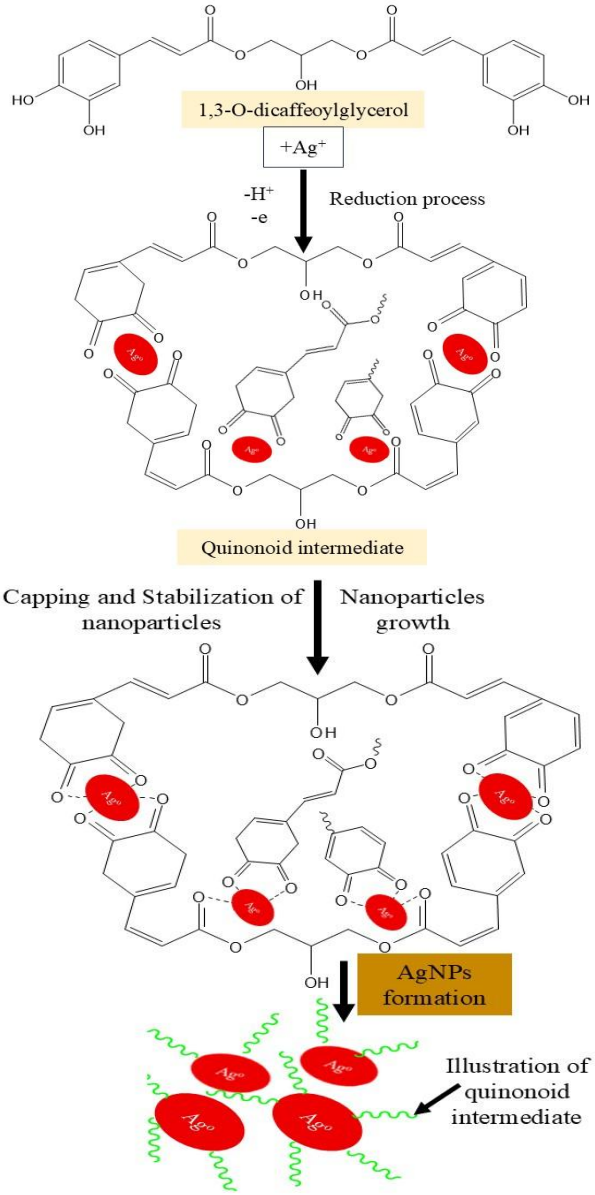

Fig. 17: The illustration of AgNP formation mediated by 1,3-O-dicaffeoylglycerol from pineapple leaf extract

4. Conclusion

This study successfully demonstrated the synthesis of silver nanoparticle-natural diatomite (AgNp-NDs) nanocomposites using two eco-friendly approaches: pineapple leaf extract (AgNp-NDs-PL) and a calcination method (AgNp-NDs-Calc). The green synthesis via pineapple leaf extract yielded smaller nanoparticles (~27 nm) for AgNP-1%-NDs-PL compared to the calcination-derived composites (~70 nm), owing to the capping and stabilizing role of phytochemicals present in the extract. Antibacterial assays revealed that AgNp-NDs-PL exhibited superior activity against *Pseudomonas aeruginosa* and *Staphylococcus aureus* at lower silver concentrations, attributed to both particle size and the synergistic effects of residual phytochemicals such as 1,3-O-dicaffeoylglycerol, as supported by molecular

simulation studies. In contrast, AgNp-NDs-Calc required higher silver content to achieve similar antibacterial performance. These findings affirm that natural diatomite waste, when valorized with agricultural biomass through a green route, provides a sustainable and effective material platform for antimicrobial applications. The results support the potential of AgNp-NDs-PL as a promising candidate for environmental and biomedical antibacterial agents aligned with circular economy strategies.

Acknowledgements

The authors would like to thank the Material Chemistry Laboratory (G-1011) Chaoyang University of Technology, Taichung, Taiwan, for research collaboration and support. Research Center for Pharmaceutical Ingredients and Traditional Medicine, Research Organization for Health, National Research and Innovation Agency, Cibinong, Indonesia for the antibacterial test.

Nomenclature

AgNp	Silver nanoparticles
AgNp-NDs-PL	Silver-diatomite nanocomposite synthesized using pineapple leaf extract
AgNp-NDs-Calc	Silver-diatomite nanocomposite synthesized via calcination
PL	Pineapple Leaf

References

1) T. Bruna, F. Maldonado-Bravo, P. Jara, and N. Caro, “Silver nanoparticles and their antibacterial applications,” Int. J. Mol. Sci., 22 (13) 7202 (2021). doi: 10.3390/ijms22137202.
2) Md. A. Huq, Md. Ashrafudoulla, M. M. Rahman, S. R. Balusamy, and Shahina Akter “Green synthesis and potential antibacterial applications of bioactive silver nanoparticles: A review,” Polymers, 14 (4) 742 (2022). doi: 10.3390/polym14040742.
3) J. B. Deshpande, S. Chakrabarty, and A. A. Kulkarni, “Heterogeneous nucleation in citrate synthesis of AgNPs: Effect of mixing and solvation dynamics,” Chem. Eng. J., 421 127753 (2021). doi: 10.1016/j.cej.2020.127753.
4) M. Mahmood, M. Abid, M. F. Nazar, M. N. Zafar, M. A. Raza, M. Ashfaq, A. M. Khan, S. H. Sumrra, and M. Zubair, “The wet chemical synthesis of surfactant-capped quasi-spherical silver nanoparticles with enhanced antibacterial activity,” Mater. Adv., 1 (7) 2332–2338 (2020). doi: 10.1039/D0MA00408A.
5) A. K. M. R. Uddin, Md. A. B. Siddique, F. Rahman, A. K. M. A. Ullah, and R. Khan, “Green synthesis of silver nanoparticles using Cocos nucifera leaf extract for enhanced antibacterial activity,” J. Inorg. Organomet. Polym. Mater., 30 (9) 3305–3316 (2020). doi: 10.1007/s10904-020-01506-9
6) Y. K. Loon, M. H. Satari, and W. Dewi, “Antibacterial effect of pineapple (Ananas comosus) extract towards Staphylococcus aureus,” Padjadjaran J. Dent., 30 (1) 1 (2018). doi: 10.24198/pjd.vol30no1.16099.
7) S. Hamdiani and Y.-F. Shih, “A green method for synthesis of silver-nanoparticles-diatomite (AgNPs-D) composite from pineapple (Ananas comosus) leaf extract,” Indones. J. Chem., 21(3) 740–749 (2022). doi:10.22146/ijc.63573
8) B. F. Alowaiesh, H. A. S. Alhaithloul, A. M. Saad, and A. A. Hassanin, “Green Biogenic of Silver Nanoparticles Using Polyphenolic Extract of Olive Leaf Wastes with Focus on Their Anticancer and Antimicrobial Activities,” Plants, 12 (6) 1410 (2023). doi: 10.3390/plants12061410.
9) V. Harish, M.M. Ansari, D. Tewari, A. B. Yadav, N. Sharma, S. Bawarig, M. -L. G. -Betancourt, A. Karatutlu, M. Bechelany, A. Barhoum, “Cutting-edge advances in tailoring size, shape, and functionality of nanoparticles and nanostructures: A review,” J. Taiwan Inst. Chem. Eng., 149 105010 (2023), doi: 10.1016/j.jtice.2023.105010.
10) S. Hamdiani, Evana, S. Hadisaputra, N. Ismillayli, I. Sumarlan, Sudirman, D. Hermanto, A. P. Sari, “Eco-Friendly Silver-Diatomite Nanocomposite Derived from Soybean Stalk Waste for Sustainable Water Purification: Antibacterial and Photocatalytic Properties,” IOP Conf. Ser.: Earth Environ. Sci., vol. 1493(1) 012011 (2025). doi:10.1088/1755-1315/1493/1/012011.
11) (11) B. Ashok, N. Hariram, S. Siengchin, A. V. Rajulu, “Modification of tamarind fruit shell powder with in situ generated copper nanoparticles by single step hydrothermal method,” J. Bioresour. Bioprod., 5 (3) 180–185 (2020). doi: 10.1016/j.jobab.2020.07.003.
12) B. Ashok, K. O. Reddy, K. Yorseng, N. Rajini, N. Hariram, S. Siengchin, and A. V. Rajulu, “Modification of natural fibers from Thespesia lampas plant by in situ generation of silver nanoparticles in single-step hydrothermal method,” Int. J. Polym. Anal. Charact., 23 (6) 509–516 (2018). doi: 10.1080/1023666X.2018.1486270.
13) K. Yorseng, S. Siengchin, B. Ashok, A. V. Rajulu, “Nanocomposite egg shell powder with in situ generated silver nanoparticles using inherent collagen as reducing agent,” J. Bioresour. Bioprod., 5 (2) 101–107 (2020). doi: 10.1016/j.jobab.2020.04.003.
14) M. H. Asraf, N. S. Sani, C. D. Williams, K. Jemon, N. A. N. N. Malek , “In situ biosynthesized silver

nanoparticle-incorporated synthesized zeolite A using Orthosiphon aristatus extract for in vitro antibacterial wound healing," Particuology, 67 27–34 (2022). doi: 10.1016/j.partic.2021.09.007.

15) M. P. Moisés, C. T. P. da Silva, C. A. A. Silva, J. G. Meneguin, G. G. Fonseca, M. R. Guilherme, A. W. Rinaldi, E. M. Girotto, E. Radovanovic, "Preparation of a sustainable Zeolite A using an agroindustry solid waste loaded with silver nanoparticles: Antimicrobial activity study," Mater. Lett., 308 131194 (2022). doi: 10.1016/j.matlet.2021.131194.
16) J. X. Chen, J. Q. Zhu, S. Y. Luo, X. X. Zhong, "A green method to the preparation of the silver-loaded diatomite with enhanced antibacterial properties," Chem. Pap., 74 (2) 8 (2019). doi:10.1007/s11696-019-00917-4
17) X. Qi, J. Chen, Q. Li, H. Yang, H. Jiang, Y. Deng, Q. Song, T. Liang, "Antibacterial silver-diatomite nanocomposite ceramic with low silver release," Water Supply, 20 (2) 633–643 (2020). doi: 10.2166/ws.2019.195.
18) A. Gil-Korilis, M. Cojocaru, M. Berzosa, C. Gamazo, N. J. Andrade, K. J. Ciuffi, "Comparison of antibacterial activity and cytotoxicity of silver nanoparticles and silver-loaded montmorillonite and saponite," Appl. Clay Sci., 240 106968 (2023). doi: 10.1016/j.clay.2023.106968.
19) S. Li, B. Mu, H. Zhang, Y. Kang, A. Wang, "Incorporation of silver nanoparticles/curcumin/clay minerals into chitosan film for enhancing mechanical properties, antioxidant and antibacterial activity," Int. J. Biol. Macromol., 223 779–789 (2022). doi: 10.1016/j.ijbiomac.2022.11.046.
20) M. El. Mouzahim, E. M. Eddarai, S. Eladaoui, A. Guenbour, A. Bellaouchou, A. Zarrouk, R. Boussen, "Effect of Kaolin clay and Ficus carica mediated silver nanoparticles on chitosan food packaging film for fresh apple slice preservation,"Food Chem., 410 135470(2023).doi:10.1016/j.foodchem.2023.135470.
21) A. Saud, S. Gupta, A. Allal, H. Preud'homme, B. Shomar, and S. J. Zaidi, "Progress in the Sustainable Development of Biobased (Nano)materials for Application in Water Treatment Technologies," ACS Omega, 9 (27) 29088–29113 (2024). doi: 10.1021/acsomega.3c08883.
22) Y. Luo, S. Shen, J. Luo, X. Wang, R. Sun, "Green synthesis of silver nanoparticles in xylan solution via Tollens reaction and their detection for Hg2+," Nanoscale, 7 (2) 690–700 (2015). doi: 10.1039/C4NR05999A.
23) J. Marczyk, K. Pławecka, M. Hebdowska-Krupa, M. Nykiel, M. Łach, "Research on diatomite from Polish deposits and the possibilities of its use," J. Achiev. Mater. Manuf. Eng., 115 (1), 5–15 (2022). doi: 10.5604/01.3001.0016.2337.
24) A. Sardo, I. Orefice, S. Balzano, L. Barra, and G. Romano, "Mini-Review: Potential of Diatom-Derived Silica for Biomedical Applications," Appl. Sci., 11 (10) 4533 (2021). doi: 10.3390/app11104533.
25) L. Gao, L. Wang, L. Yang, Y. Zhao, N. Shi, C. An, Y. Sun, J. Xie, H. Wang, Y. Song, Y. Ren, "Preparation, characterization and antibacterial activity of silver nanoparticle/graphene oxide/diatomite composite," Appl. Surf. Sci., 484 628–636 (2019), doi: 10.1016/j.apsusc.2019.04.153.
26) K. H. Min, J. W. Shin, M. -R. Ki, S. P. Pack, "Green synthesis of silver nanoparticles on biosilica diatomite: Well-dispersed particle formation and reusability," Process Biochem., 125 232–238 (2023). doi: 10.1016/j.procbio.2022.12.018.
27) Accelrys Software Inc. (2011). Materials Studio, Version 7.0. San Diego: Accelrys Inc.
28) C. Ma, S. Xiao, Z. Li, W. Wang, and L. Du, "Characterization of active phenolic components in the ethanolic extract of Ananas comosus L. leaves using high-performance liquid chromatography with diode array detection and tandem mass spectrometry," Journal of Chromatography A, 1165 (1–2) 39–44 (2007). doi: 10.1016/j.chroma.2007.07.060.
29) O. Pryshchepa, P. Pomastowski, B. Buszewski, "Silver nanoparticles: Synthesis, investigation techniques, and properties," Adv. Colloid Interface Sci., 284 102246 (2020). doi: 10.1016/j.cis.2020.102246.
30) Z. Hu, S. Zheng, J. Li, S. Zhang, M. Liu, Z. Wang, J. Li, H. Sun, "Pore structure and surface properties of diatomite with mechanical grinding and its influence on humidity control performance," Physicochem. Probl. Miner. Process., 58 (6) 153509 (2022). doi: 10.37190/ppmp/153509.
31) S. Kasim, S. Dali, and M. Rahmah, "Synthesis of silver nanoparticles using bioreductors from clove leaf extract (Syzygium aromaticum) and test of its antibacterial activity," J. Phys. Conf. Ser., 1763 (1) 012051 (2021). doi: 10.1088/1742-6596/1763/1/012051.
32) J. Fowsiya and G. Madhumitha, "Biomolecules Derived from Carissa edulis for the Microwave Assisted Synthesis of Ag2O Nanoparticles: A Study Against S. incertulas, C. medinalis and S. mauritia," J. Clust. Sci., 30 (5) 1243–1252 (2019). doi: 10.1007/s10876-019-01627-3.
33) S. P. Diggle and M. Whiteley, "Microbe Profile: Pseudomonas aeruginosa: opportunistic pathogen and lab rat: This article is part of the Microbe Profiles collection.," Microbiology, 166 (1) 30–33 (2020). doi: 10.1099/mic.0.000860.
34) M. E. Perez, R. G. Fenoll, S. M. Bayo, R. M. M. Álvarez, V. F. Millán, M. C. V. Usón, M. P. P.

Ruiz, J. M. A. Mainar, M. C. M. Jiménez, C. R. Paesa, “Impact of Staphylococcus aureus bacteremia in COVID-19 patients,” Rev. Esp. Quimioter., 35 (5) 468–474 (2022). doi: 10.37201/req/022.2022.

35) I. Falces-Romer, I. Bloise, J. García-Rodríguez, E. Cendejas-Bueno, “Staphylococcus aureus bacteremia in patients with SARS-CoV-2 infection,” Med. Clínica Engl. Ed., 160 (11) 495–498 (2023). doi: 10.1016/j.medcle.2023.05.007.

36) A. Baran, C. Keskin, M. F. Baran, I. Huseynova, R. Khalilov, A. Eftekhari, S. Irtegun-Kandemir, D. E. Kavak, “Ecofriendly Synthesis of Silver Nanoparticles Using Ananas comosus Fruit Peels: Anticancer and Antimicrobial Activities,” Bioinorganic Chemistry and Applications, 2021 1–8 (2021). doi: 10.1155/2021/2058149.

37) I. Wojtczak, W. Brzozowska, V. Railean, Z. Bekissanova, G. Trykowski, and M. Sprynskyy, “Diatomaceous Biosilica Doped with Heteroepitaxially Growing Ag/AgCl/CeO2 Composite Nanoparticles: Synthesis, Characterisation and Antibacterial Application,” J Clust Sci, 35 (2) 429–442 (2024). doi: 10.1007/s10876-023-02492-x.

38) S. A. Hashib, N. F. M. Zain, and M. N. M. Zain, “Green synthesis of silver nanoparticles using pineapple peel extract and the study of their antibacterial activity,” J. Fundam. Appl. Sci., 10 (5) 129–139 (2018).